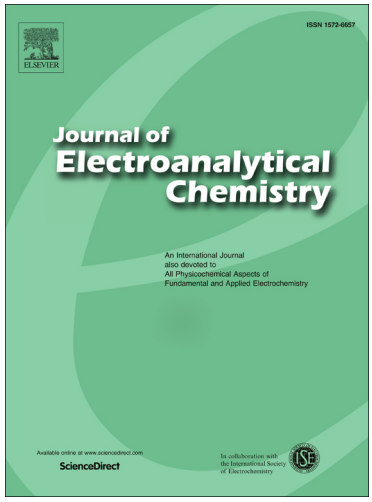

Comparative electrochemical performance of electrodeposited polypyrrole in protic and aprotic ionic liquids

R.A. Fernández, T.M. Benedetti, R.M. Torresi

PII: S1572-6657(14)00206-9
DOI: http://dx.doi.org/10.1016/j.jelechem.2014.05.020
Reference: JEAC 1674

To appear in: *Journal of Electroanalytical Chemistry*

Received Date: 20 March 2014
Revised Date: 8 May 2014
Accepted Date: 19 May 2014

Please cite this article as: R.A. Fernández, T.M. Benedetti, R.M. Torresi, Comparative electrochemical performance of electrodeposited polypyrrole in protic and aprotic ionic liquids, *Journal of Electroanalytical Chemistry* (2014), doi: http://dx.doi.org/10.1016/j.jelechem.2014.05.020

Comparative electrochemical performance of electrodeposited polypyrrole in protic and aprotic ionic liquids

R.A Fernández, T. M. Benedetti, R. M. Torresi*

Instituto de Química, Universidade de São Paulo, CP 26077, 05513-970 São Paulo, Brazil

Abstract:

Polypyrrole (Ppy) thin films were obtained by pyrrole (py) electropolymerization in ionic liquid (IL) media. The charge compensation dynamics as well as the electrochromic behaviour of the obtained films were studied in two ILs with similar structures, being one containing -CH_3 (aprotic IL) and the other containing -H (protic IL) attached to the ethylimidazolium cation.

The results obtained with quartz crystal microbalance with dissipation combined with cyclic voltammetry have shown that in spite of the presence of protons in the PIL, which could favour both electropolymerization and electrochemistry of Ppy in this media, these processes are more effective in the aprotic IL, leading us to conclude that other factors must be take into account when choosing the most appropriated IL as electrolyte. Also, electrochemical reactions in both ILs were successfully associated to the transformation of chromogenic species by evaluating the electrochromic activity of the polymeric films.

Keywords: conducting polymers, polypyrrole, quartz crystal microbalance, electroctrochromism, protic ionic liquids, electropolymerization

*Corresponding author: rtorresi@iq.usp.br

1. Introduction

Protic ionic liquids (PILs) are ionic liquids (ILs) which are formed through proton transfer from a Brønsted acid to a Brønsted base, resulting in materials bearing protons attached to their cations. They have some characteristic properties of the aprotic ionic liquids (AILs), ie. high ionic conductivity and low vapour pressure, depending on the extent of proton transfer, but can be easier obtained when compared to the aprotic analogous [1].

Another particular interest in this subclass of IL is related to the ability to conduct protons under anhydrous conditions [2], and it has been growing interest to understand the relationship between its ionicity and several physicochemical properties [3,4]. Recent contributions have shown that the PILs are promising electrolytes for improving electrochemical performance of modified electrodes in applications such as electrolytes for safer lithium-ion batteries [5] solar cells [6] and non-humidified fuel cells. [7]

Another interesting application could be as electrolytes for electropolymerization of conducting polymers. Previous contributions have shown successful electropolymerization of conducting polymers in AIL: in reference 8, pyrrole (py) was electropolymerized in an AIL containing the anion hexafluorophosphate, showing good polymerization rates and electrochemical response toward ascorbic acid and dopamine; in reference 9, it was possible to obtain electropolymerized thin films of polyaniline in AIL based electrolyte and the addition of an acid to the electrolytic media promoted the conversion from the base (non-conducting) to the salt (conducting) form. Once PILs already possess protons available in their cations, they are interesting electrolytes for the obtention of thin films of conducting polymers [10]. In fact, anilinium nitrate salt was dissolved in a PIL and in an AIL, and electropolymerization has shown superior performance when the PIL was employed [11]. Concerning polypyrrole (Ppy), in

general, electropolymerization can undergo at any pH, being favourable in acid conditions although very low pH values can result in films with low conductivity [12].

As far as we are concerned, electropolymerization and electrochemistry of Ppy were only conducted in AIL [13-18]; so that, in the present work, the factors affecting the electropolymerization of py to produce the conducting polymer Ppy, as well as the role of the species participating in the charge balancing process of the obtained Ppy films in both AIL and PIL were studied. For that, two structurally similar ILs, differing only by the presence of $-CH_3$ (AIL) or -H (PIL) attached to the cation ethylimidazolium were employed. Additionally, the electroctrochromic behaviour of these systems was evaluated and discussed.

2. Experimental:

The PIL, ethyl-imidazolium bis(trifluoromethylsulfonyl)imide ($HEITf_2N$) was obtained by acid-base reaction. Equimolar amounts of the acid, trifluoromethanesulfonimide (HTf_2N - Fluka), dissolved in dichloromethane were added slowly (at a speed of 1 mL min^{-1}) to previously distilled 1-ethyl-imidazole (Aldrich) under stirring in a round bottom flask placed into ice bath. The temperature during the reaction was maintained below 40°C. The AIL, 1-ethyl-3-methylimidazolium bis(trifluoromethylsulfonyl) imide ($EMITf_2N$) was obtained by mixing aqueous solutions of 1-ethyl-3-methylimidazolium bromide (Aldrich) and lithium bis(trifluoromethanesulfonyl)imide ($LiTf_2N$ - Aldrich), followed by purification processes [19]. The water content, determined by Karl-Fischer titration using a Karl-Fischer Coulometer (Metrohm) was 2000 ppm for the PIL and the water content of the AIL was adjusted to the same value for comparison purposes. Remaining water becomes strongly coupled to PILs by hydrogen bond and is more difficult to be

removed when compared to AILs [20]. The viscosities of both ILs were measured with an Anton Paar viscosimeter model SVM 3000, being the values obtained at 25°C 45.3 mPa s for the AIL and 21.3 mPa s for the PIL. The chemical structures of the two ILs are disclosed in Figure 1.

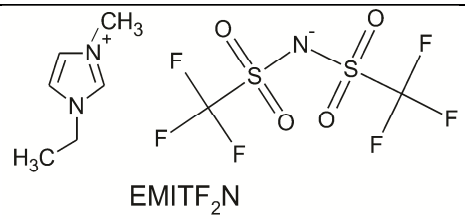

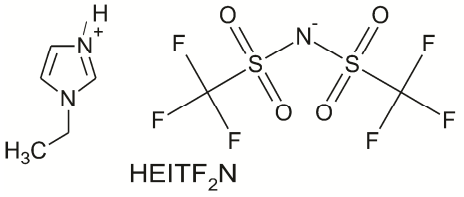

Figure 1: Chemical structure of ILs: 1-ethyl-3-methyl-imidazolium bis(trifluoromethylsulfonyl)imide ($EMITf_2N$) and 1-ethyl-imidazolium bis(trifluoromethylsulfonyl)imide ($HMITf_2N$)

All electrochemical measurements were performed with an AUTOLAB PGSTAT 30 potentiostat, using Pt mesh and Ag wire as counter and reference electrodes respectively and voltammetric studies of ILs containing Ferrocene/Ferrocenium (Fc/Fc^+) as an internal reference were previously performed in order to define the potential windows.

Ppy films were electropolymerized at constant current in 0.1 mol L^{-1} of distilled py (Aldrich) mixed with both ILs. The films were deposited over glass substrates covered with indium tin oxide (ITO) (Delta Technologies) or AT-cut 5 MHz piezoelectric quartz crystals (14 mm diameter) coated with platinum (Qsense).

For the spectro-electrochemical studies, transmittance-potential profiles were obtained simultaneously with cyclic voltammetry. As light source an incident light (electromagnetic radiation) spot at a specified wavelength generated by a solid-state

light source (World Precision Instruments) was used. Optical fibers were used to transport the light that passes through the sample from the electrochemical cell to a photodiode amplifier PDA1 (World Precision Instruments), linked to an ADC port in the potentiostat.

For the electrogravimetric studies, the cyclic voltammetry data was simultaneously recorded with frequency and dissipation changes using a Quartz Crystal Microbalance with Dissipation (QCM-D) from Q-Sense (model E4). An electric field applied to the quartz crystal causes it to oscillate at a specific frequency and when the oscillation frequency change is only related with mass change on the quartz surface (i.e. no viscoelastic changes), they are related through the Sauerbrey equation: $\Delta f = -\Delta m / CA$ [21], where Δf is the measured shift in frequency in Hz, Δm is the mass change, A is the active area of the quartz crystal and C is the theoretical mass sensitivity. C was calculated by relating the charge and mass change during electrodeposition of cooper and using the quartz crystal parameters the value obtained was 17.7 ng cm^{-2} Hz^{-1}[22]. Cooper was chose because its reduction potential is higher enough to disregard the water reduction, so the charge can be directly related with the deposited mass. Nevertheless, when the frequency change is also associated with viscoelastic changes in the film, the Sauerbrey equation can no longer be applied and an appropriated viscoelastic model must be used [23].

Atomic force microscopy (AFM) images were taken with a Pico SPM-LE molecular imaging system with cantilevers operating in the intermittent contact mode (AAC mode), slightly below their resonance frequency of approximately 305 kHz in the air. Topographic images refer to scan areas of 25 μm x 25 μm and 2 μm x 2 μm. Image processing and root mean square roughness parameter (Rq) were performed with Pico Scan Software. Rq is the statistical function that represents the standard deviation of the

distribution of surface heights [24]. Each film obtained at different current densities was analyzed at four different topographic positions on the surface.

3. Results and discussion

3.1 Electropolymerization of py in ILs

The frequency and dissipation changes at different overtones were monitored by QCM-D during the electropolymerization of py at constant current of 190 μA cm^{-2} in both PIL and AIL. The frequency variation during the process is the same independently on the overtone and the obtained data for the 3rd one is presented in figures 2a and 2b as an example. In addition, there is no dissipation change during the measuring, which means that the obtained films are thin enough to be considered as rigid ones and Sauerbrey equation can be employed for obtention of mass of the polymer [18]. The mass variation as a function of time during the electrodeposition in both AIL and PIL are presented in figure 2c.

In spite of similar polymerization rate for both ILs, it was not possible to obtain Ppy films with good reproducibility in the protic one. When the monomer is added to the PIL, the mixture acquires a dark yellow coloration after few minutes being brown after one day possibly due chemical polymerization of py in the PIL as it has been previously observed in strong acid solutions such as calix-6-arenehexasulfonic acid [25] and hydrochloric acid [26].

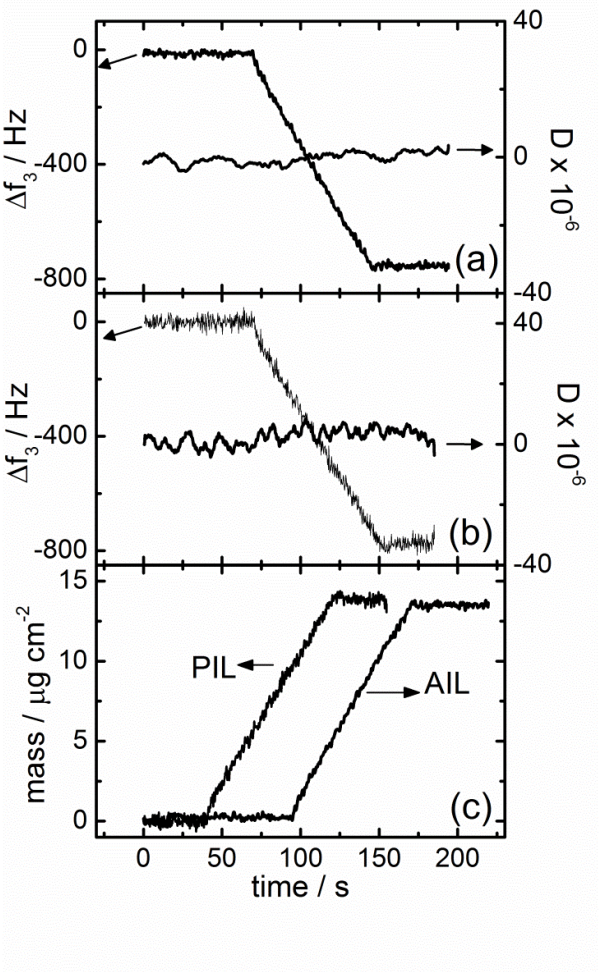

Figure 2: 3rd overtone frequency and dissipation changes in $EMITf_2N$ (a) and $HEITf_2N$ (b) and mass variation as a function of time (c) during electropolymerization of pyrrole at constant current. Applied current density: 190 µA cm^{-2}.

On the other hand, thin and uniform Ppy films were obtained with good reproducibility in the AIL. The electropolymerization of py was run galvanostatically at different current densities ranging from 65 µA cm^{-2} to 190 µA cm^{-2} and it was monitored by QCM-D measurements. In Figure 3a the mass variations at the different current densities during deposition in the $EMITf_2N$ are shown. During the electrochemical synthesis, the anions Tf_2N^- are incorporated (p-doping) into the polymer structure to balance the positive charges present along the polymer backbone as previously observed for a similar AIL containing the same cation and the $CF_3SO_3^-$ anion

[27]. During the polymer synthesis a constant potential value of ca. 0.80 V (vs. Fc/Fc^+) is reached for all employed current densities and the mass increases linearly with time until the current supply is stopped. These results indicate that, in the range of current densities employed, higher applied currents produce higher growth rates. Actually, the different slope values at different deposition times correspond to the same total charge, so as predictable, mass variation as function of the charge at different applied current densities automatically collapses in one curve as it is in Figure 3b. Therefore, knowing the applied charge during the electropolymerization of py, is possible to estimate the mass of the deposited film independently of the applied current density.

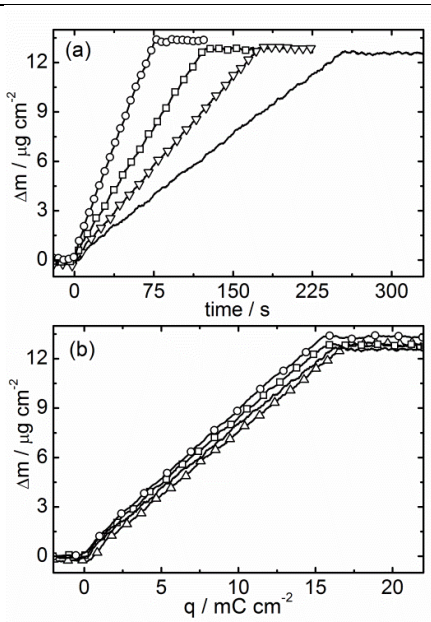

Figure 3: EQCM-D mass variation response recorded during the galvanostatic electropolymerization of PPy films in the $EMITf_2N$ at j = 190 μA cm^{-2} (○) ; j = 130 μA cm^{-2} (□) ; j = 95 μA cm^{-2} (Δ) and j = 65 μA cm^{-2} (—) as a function of time (a) and as a function of charge (b).

Dark coloured films were obtained indicating that the polymer is in its oxidized form [28] and from the slope of the mass vs. charge plot is possible to obtain the doping degree of the obtained polymer as follows [28, 29]: the total charge q associated with the polymerization reaction followed by film oxidation can be represented by:

$$q = nF(2 + x) \quad (1)$$

where F is the Faraday constant, n the number of moles of monomer, and x represents the degree of doping.

Accordingly to the general polymerization reaction represented by the following chemical equation:

$$[py(A^{1-})_x]_n + py + xA^{1-} \rightarrow [py(A^{1-})_x]_{n+1} + 2H^{1+} + (2 + x)e^{1-} \quad (2)$$

The total mass change throughout these two processes can be described by:

$$\Delta m = n\left(M_{py} + xM_{A^-} - 2M_{H^+}\right) \quad (3)$$

where M_{py}, M_A and M_H are the molar mass of py, the anion Tf_2N^- and protons, respectively. With the experimental slope $\Delta m/\Delta q$ = 0.77 mg C^{-1} obtained from Figure 3b, and combining the later expressions (equation 4):

$$\frac{n(M_{py}+x^{-1}M_{A^-}+M_{H^+})}{nF(2+x^{-1})} = 0.77 \times 10^{-3}\,\mathrm{g\,C^{-1}} \quad (4)$$

it is possible to estimate a doping level of 40 % for the anion incorporation process during the electropolymerization, which is higher than typically observed in conventional electrolytic media (i.e. 25 to 33%) [28-30] including for Ppy obtained in $LiClO_4$ aqueous electrolyte [31], for example.

As the electronic properties of Ppy films are associated to their morphology [32, 33] AFM images were obtained and a surface roughness analysis was done. Figure 4 shows AFM images of Ppy films electrodeposited at two different current densities (65 and 190 μA cm^{-2}) as examples. From the images it is possible to observe the formation of a smooth surface in both cases. AFM images of four different regions of each film were taken in order to obtain the Rq values, which was (4.0 ± 0.5) nm for all the films. The films grown in IL media present a smoother surface morphology than usually observed in conducting polymers obtained in non-aqueous conventional solvent systems

[34] and the analysis of the surface morphology is in agreement with previous works showing that larger doping anions provide more uniform Ppy film structures [34, 35].

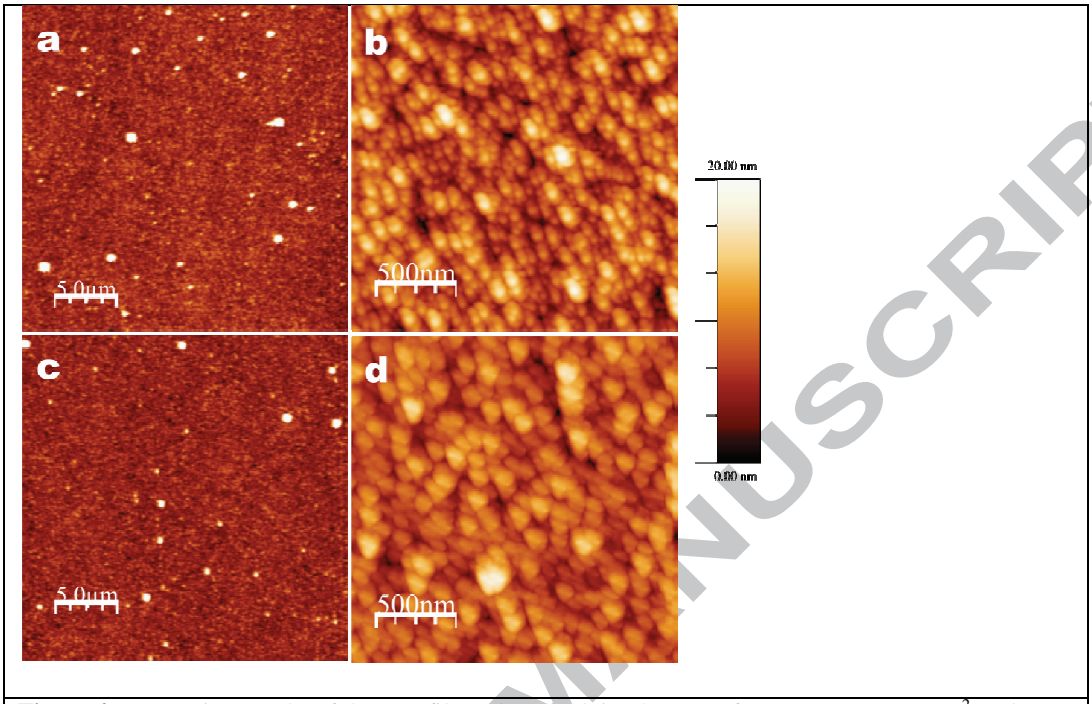

Figure 4: AFM micrographs of the PPy films deposited in the $EMITf_2N$ at $j = 130$ µA cm^{-2}: 25 µm x 25 µm (a) and 2 µm x 2 µm (b); and at $j = 95$ µA cm^{-2}: 25 µm x 25 µm (c) and 2 µm x 2 µm (d).

3.2. Charge compensation analysis

The obtained Ppy films were electrochemically characterized in both AIL and PIL. In order to understand the species that are taking part in the charge balancing process, the cyclic voltammetry was combined with QCM-D measurements. Figure 5 shows the potentiodynamic profiles normalized by the mass of the formed films in AIL, and cycled in AIL and PIL as electrolytes at 50 mV s^{-1}. Control experiments, in which bare Pt substrates were cycled in the ILs have shown that the employed electrolytes are not electrochemically active in these potential windows range (data not shown). In the AIL, two cathodic and two anodic current peaks are observed at −0.6 V and −1.0 V and -0.7 V and -0.2 V respectively; while in the PIL two cathodic current peaks at 0.1 V and -0.3 V and only one anodic peak at -0.1 V are observed in the applied potential range.

Considering the reduction processes, their happen at more negative potentials when the AIL is employed which is in accordance with what has been observed in aqueous solutions with different pHs [36]. This behavior is attributed to different kinds of reduction process when it happens in acid or neutral/alkaline media. In fact, this assumption can be corroborated when one analyze the voltammograms together with the mass change, as it can be observed in figure 6a for the AIL and figure 6b for the PIL.

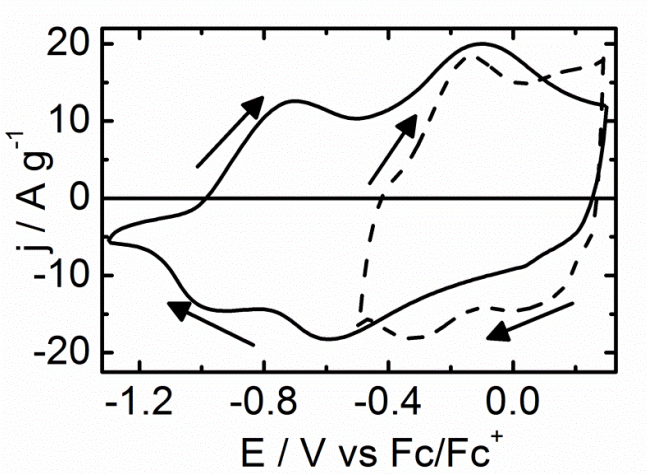

Figure 5: Cyclic voltammograms for PPy, cycled in $EMITf_2N$ (full line) and $HEITf_2N$ (dashed line) as electrolytes. Scan rate: 50 m V s^{-1}.

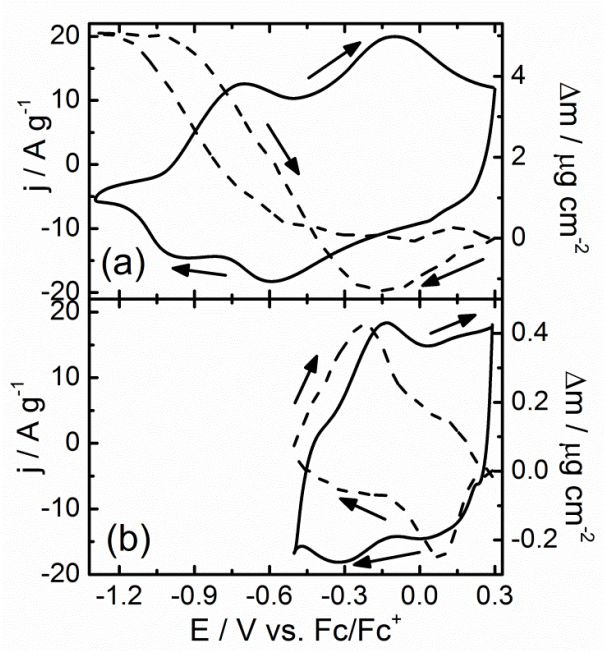

Figure 6: current (full line) and mass change (dashed line) as a function of potential of Ppy in $EMITf_2N$ (a) and $HEITf_2N$ (b). Scan rate: 50 m V s^{-1}.

In both electrolytes, during the reduction, firstly a mass decrease is observed followed by the gain of mass indicating release of anions followed by insertion of cations. However, the contribution of cations is significantly higher in the AIL electrolyte while in the PIL, the participation of anions in the charge compensation process is more important.

One hypothesis for this observation is that the Ppy film is protonated when it is immersed in the PIL facilitating the insertion of anions instead of cations during the charge compensation, while in the AIL, as the film is deprotonated, the charge compensation will be done by the positive ions. However, a more detailed data analysis taking into account the molar mass of IL species combined with a charge compensation analysis of the film reveals a preponderance of cation injection flux over anion ejection during all negative potential scan in both ILs as it is shown in the following paragraphs.

Charge compensation dynamics in the system can be solved considering mass and charge balance into the polymer film. Thus, considering the participation of positive and negative ions at the polymer/solution boundary and the mass change of the Ppy film, the exchange of cations and anions were calculated for the PIL and the AIL as electrolytes. Combining mass and charge balances, the amount of moles exchanged (ξ) as a function of applied potential can be obtained [28, 29, 37]. Also, individual cation (j_{cation}), and anion charge fluxes expressed in terms of current (j_{ion}) as a function of applied potential (E) can be calculated using the following expression (equation 5):

$$j_{ion(E)} = \frac{d\xi_{ion(E)}}{dt} \qquad (5)$$

where ξ_{ion} must be ξ_{cation} or ξ_{anion} to obtain j_{cation} or j_{anion}, being the signal positive or negative for ion insertion or ejection respectively. Figure 7a and 7b show the potentiodynamic j/E profiles for PPy films cycled in both ILs, also presenting calculated individual ions contribution to total charge compensation. These results show that j_{cation} is higher than $j_{anion,}$ in all potential range for both electrolytes, driving to the conclusion that the charge compensation processes are mainly achieved by the ejection/insertion of positive ions in both ILs. So, mass profile have to be carefully read because of the difference in molar mass of the participating anions (Tf_2N^- = 280 g mol^{-1}) and cations (EMI^+ = 111 g mol^{-1} and HEI = 99 g mol^{-1}). In fact, although the same involved current densities, the mass change for the experiment performed in the PIL is ten times lower than the one done in the AIL (see figure 6). In this way, in the case of the PIL, is relevant to note that in spite of the Ppy being protonated when immersed in the PIL, the charge compensation during redox processes occurs mainly by the ejection/insertion of protons into the polymeric matrix with cycling. This observation can be ascribed to the fact that the protons are smaller than the other ionic species, facilitating its insertion/deinsertion for charge compensation.

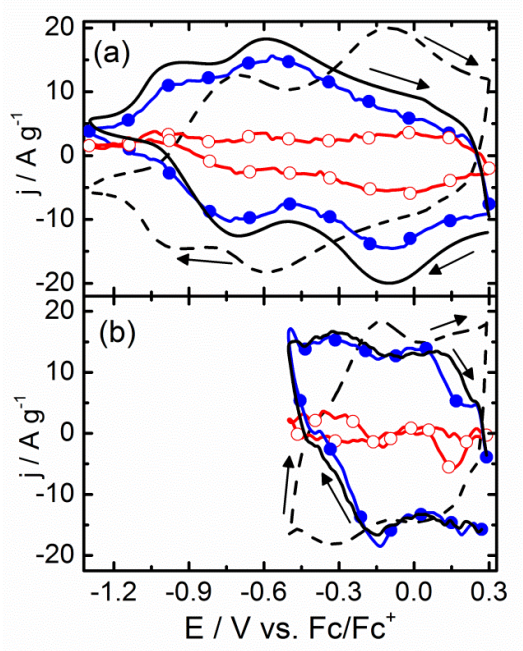

Figure 7: Potentiodynamic *j*/*E* profiles (dashed line) for PPy films cycled in $EMITf_2N$ (a) and $HEITf_2N$ (b), showing calculated individual ions contribution to total charge compensation. Cations/H_3O^+ flux (full blue circle), anions flux (open red circle), and total ionic flux (full black line); scan rate: 50 m V s^{-1}.

The specific capacitance and the energy densities of these films were calculated by integration of current vs. time profile from the cyclic voltammograms, being the values obtained 231 F g^{-1} and 281 F g^{-1} for the AIL and the PIL respectively. These are relatively high values compared with PPy based electrode materials for supercapacitors informed in literature [38, 39]. Even though, in spite of the higher capacitance in the PIL, the wider electrochemical window in the AIL provides higher energy densities (*E*) accordingly to the following expression (equation 6):

$$E = CV^2 \qquad (6)$$

where *C* is the specific capacitance and *V* is the electrochemical window [40]. The calculated energy densities values are 163 W h kg^{-1} and 50 W h kg^{-1} for the AIL and the PIL respectively. These results show that, when selecting the proper electrolyte, not only the capacitance values must be take into account, but also the working electrochemical window in order to reach high energy density levels.

3.3. Electrochromic behaviour

For the electrochromic studies, cyclic voltammetry were performed simultaneously with monitoring of absorbance changes as function of applied potential at two fixed wavelengths: 660 nm (red) and 480 nm (blue) for both electrolytes (figures 8 a and 8b). The studies made at the different wavelengths are important once the different species at different oxidation states absorb at different regions in the spectrum. In the UV-Vis spectrum of Ppy films a band at 430 nm is present when it is in the reduced form. When it is oxidized, this band vanishes giving rise to a broad band from 600 to 800 nm. These bands were previously attributed in literature to the presence of polaron and bipolaron states in the doped form of Ppy [41-44].

The change from dark coloured to pale yellow corresponding to the transition from oxidized to neutral Ppy was observed when the potential was varied in the negative direction in both ILs as electrolytes. The process is accompanied by the decrease of absorbance at 600 nm while it increases at 480 nm. It has to be notice that Ppy films were deposited over glass slides covered with ITO transparent working electrodes for these measurements, which is the reason why the voltammograms profile are different with respect to the former ones (performed over the quartz sensors covered with platinum). The platinum can act as an electrocatalyst, changing the reduction/oxidation potentials.

When the colour change and charge transfer reaction happen simultaneously, the differential of the absorbance curve as function of applied potential (dA/dt vs. E) corresponds to the voltammetric profile [45]. Thus, when the superposition of dA/dt curves with the cyclic voltammograms is observed it means that the electrochemical reaction is exclusively related to the transformation of chromogenic species.

In figure 8c, by observing the curves at different wavelengths, we notice that the one at 660 nm (red colour) follows the cyclic voltammograms profile in the AIL which shows that the number of oxidized species that absorbs at this wavelength are increasing during the positive potential scan. At 480 nm (blue colour) the opposite behaviour is observed, indicating that the neutral species that absorbs at this wavelength are disappearing during the oxidation. The same behaviour is observed for the experiments done in the PIL as electrolyte (figure 8d). Once the electrochemical and the electrochromic reactions are observed at practically the same potential values, it is worth to affirm that they are directly associated and happening at practically the same rate.

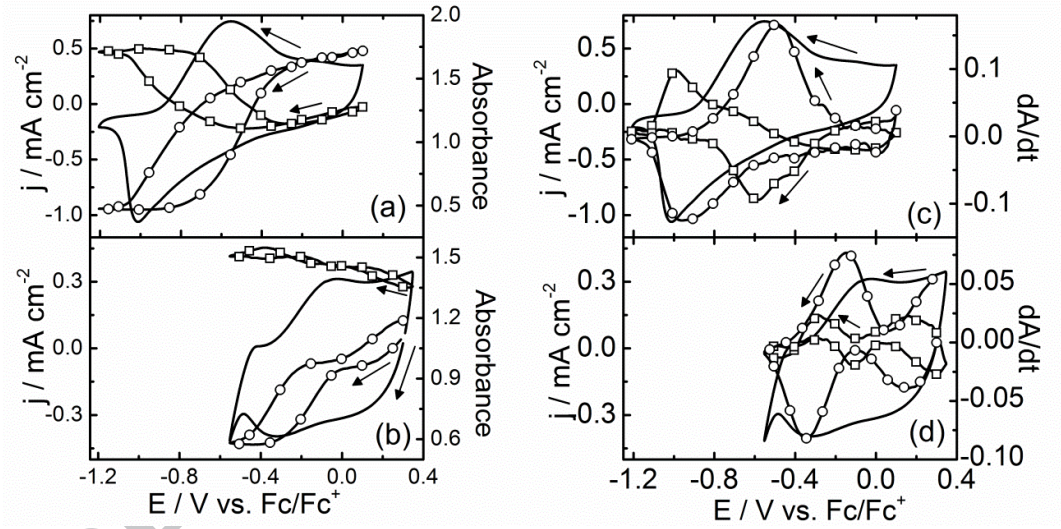

Figure 8: Cyclic voltammogram (full line) Absorbance (a and b) and *dA/dt* (c and d) vs applied potential at 480 nm (open square) and at 660 nm (open circle) for PPy in $EMITf_2N$ (a and c) and $HEITf_2N$ (b and d). Scan rate: 50 m V s^{-1}.

Conclusions

The electrochemistry of Ppy in a protic and an aprotic IL with similar structures was evaluated. It was not possible to obtain uniform Ppy thin films with good reproducibility due the very low stability of the py/PIL mixture. However, thin and

uniform Ppy film were obtained in the AIL, whose charge compensation process was studied in both protic and aprotic ILs.

The electrochemical characterization has shown that charge compensation process is mainly done by the positive ions, being the protons the main responsible for the process in the PIL. Although the higher capacitance achieved with the PIL, the performance in terms of energy density is better with the AIL due its wider electrochemical window. Concerning the mechanisms of color change, it is reversibly associated with the redox processes in both protic and aprotic ILs as it was observed by the spectro-electrochemical studies.

As general conclusion, although PILs being promising electrolytes for both electropolymerization and charge compensation processes for conducting polymers, it has been shown that both obtention and electrochemistry of Ppy is more effective in the analogous aprotic IL. Several aspects beyond the presence of protons must be take into account when choosing the most appropriated IL as electrolyte.

Acknowledgements

Authors thanks FAPESP (Proc. 09/53199-3), CNPq and CAPES for financial support. R.A.F and T.M.B thank FAPESP (Proc. 11/20711-3 and 12/02117-0) for the fellowships granted.

References:

[1] M. Yoshizawa, W. Xu, C. A. Angell, J. Am. Chem. Soc. 125 (2003) 15411–15419.

[2] C. Zhao, G. Burrell, A. a J. Torriero, F. Separovic, N. F. Dunlop, D. MacFarlane, A. M. Bond, J. Phys. Chem. B, 112 (2008) 6923–6936.

[3] J. Stoimenovski, E. I. Izgorodina, D. MacFarlane, Phys. Chem. Chem. Phys. 12 (2010) 10341–10347.

[4] J-P. Belieres, C. A. Angell, J. Phys. Chem. B, 111 (2007) 4926–4937.

[5] S. Menne, J. Pires, M. Anouti, a. Balducci, Electrochem. Commun. 31 (2013) 39–41.

[6] A. Abate, D. J. Hollman, J. Teuscher, S. Pathak, R. Avolio, G. D. Errico, G. Vitiello, S. Fantacci, H. J. Snaith, J. Am. Chem. Soc. 135 (2013) 13538–13548.

[7] T. Yasuda, M. Watanabe, MRS Bull. 38 (2013) 560–566.

[8] A. Zhang, J. Chen, D. Niu, G. G. Wallace, J. Lu, Synth. Met. 159 (2009) 1542–1545

[9] F. F. C. Bazito, L. T. Silveira, R. M. Torresi, S. I. Cordoba de Torresi, Phys. Chem. Chem. Phys., 10 (2008) 1457–1462.

[10] J. M. Pringle, M. Forsyth, D. R. Macfarlane, in Electrodeposition from Ionic Liquids (Eds.: F. Endres, D.R. MacFarlane, A. Abbott), WILEY-VCH Verlag GmbH & Co, Weinheim, 2008, pp. 167–211.

[11] G. A. Snook, T. L. Greaves, A. S. Best, J. Mater. Chem., 21 (2011) 7622-7629

[12] S. Sadki, P. Schottland, N. Brodie, and G. Sabouraud, Chem. Soc. Rev., 29 (2000) 283–293

[13] G. Sigircik, T. Tuken, M. Erbil, Mater. Chem. Phys., 138 (2013) 823-832

[14] S. Ahmad, S. Sen Gursoy, S. Kazim, A. Uygun, Sol. Energy Mater. Sol. Cells, 99 (2012) 95-100.

[15] G. Zhang, H. Zhou, J. Zhang, X. Han, J. Chen, Y. Kuang, J. Appl. Polym. Sci., 125 (2012) 2342-2347.

[16] G. A. Snook, A. S. Best, J Mater Chem, 19 (2009) 4248-4254.

[17] J. M. Pringle, O. Winther-Jensen, C. Lynam, G. G. Wallace, M. Forsyth, D. R. MacFarlane, Adv. Funct. Mater., 18 (2008) 2031-2040.

[18] J. M. Pringle, O. Ngamna, C. Lynam, C., G. G. Wallace, M. Forsyth, D. R. MacFarlane, Macromolecules, 40 (2007) 2702-2711.

[19] T. M. Benedetti, F. F. C. Bazito, E. A. Ponzio, R. M. Torresi, Langmuir, 3602 (2008) 3602-3610

3610.

[20] G. L. Burrell, I. M. Burgar, F. Separovic, N. F. Dunlop, Phys. Chem. Chem. Phys., 12 (2010) 1571–1577.

[21] G. Sauerbrey, Z. Phys. A: Hadron Nucl., 155 (1959) 206–222.

[22] L. E. Valenti, V. L. Martins, E. Herrera, R. M. Torresi, C. E. Giacomelli, J. Mater. Chem. B, 1 (2013) 4921-4931.

[23] T. M. Benedetti, R. M. Torresi, Langmuir 29 (2013) 15589-15595.

[24] E. S. Gadelmawla, M. M. Koura, T. M. a. Maksoud, I. M. Elewa, H. H. Soliman, J. Mater. Process. Technol., 123 (2002) 133–145.

[25] D. A. Reece, J. M. Pringle, S. F. Ralph, G. G. Walllace, Macromolecules 38 (2005) 1616-1622.

[26] S. J. Hawkins, N. M. Ratcliffe, J. Mater. Chem., 10 (2000) 2057-2062.

[27] Sekiguchi, K.; Atobe, M.; Fuchigami, T., Electrochem Commun., 4 (2002) 881-885.

[28] R. C. D. Peres, M. A. De Paoli, R. M. Torresi, Synth. Met., 48 (1992) 259–270.

[29] G. Maia, R. M. Torresi, E. A. Ticianelli, F. C. Nart, J. Phys. Chem., 100 (1996) 15910–15916.

[30] S. Sadki, P. Schottland, N. Brodie, and G. Sabouraud, Chem. Soc. Rev., 29 (2000) 283–293.

[31] I. Villarreala, E. Moralesa, T.F. Oterob, J.L. Acosta, Synth Met, 123 (2001) 487–492.

[32] J. Pringle, J. Efthimiadis, P. Howlett, D. MacFarlane, A. Chaplin, S. Hall, D. Officer, G. Wallace, M. Forsyth, Polymer, 45 (2004) 1447–1453.

[33] T. Silk, Q. Hong, J. Tamm, R. G. Compton, Synth. Met., 93 (1998) 59–64.

[34] F. T. A. Vork, B. C. A. M. Schuermans, E. Barendrecht, Electrochim. Acta, 35 (1990) 567–575.

[35] U. Paramo-Garcia, J. G. Ibanez, N. Batina, Int. J. Electrochem. Sci., 8 (2013) 2656–2669.

[36] Q. Xie, S. Kuwabata, H. Yoneyama, J. Electroanal. Chem., 420 (1997) 219-225.

[37] E. P. Cintra, R. M. Torresi, G. Louarn, S. I. Córdoba de Torresi, Electrochim. Acta, 49 (2004) 1409–1415.

[38] K. Jurewicz, S. Delpeux, V. Bertagna, F. ˜Béguin, E. Frackowiak, Chem. Phys. Lett., 347 (2001) 36–40.

[39] M. D. Ingram, H. Staesche, K. S. Ryder, Solid State Ionics, 169 (2004) 51–57.

[40] T. M. Benedetti, V. R. Gonçales, S. I. Córdoba de Torresi, R. M. Torresi, J. Power Sources, 239 (2013) 1–8.

[41] J. L. Bredas, G. B. Street, Acc. Chem. Res., 1305 (1985) 309–315.

[42] G. Zotti, G. Schiavon, Synth. Met., 30 (1989) 151–158.

[43] T. F. Otero, M. Bengoeche, Langmuir, 15 (1999) 1323–1327.

[44] J. Arjomandi, A.-H. A. Shah, S. Bilal, H. Van Hoang, R. Holze, Spectrochim. Acta. A. Mol. Biomol. Spectrosc. 78 (2011) 1–6.

[45] M. Malta, E. R. Gonzalez, R. M. Torresi, Polymer, 43 (2002) 5895–5901.

Fig. 4

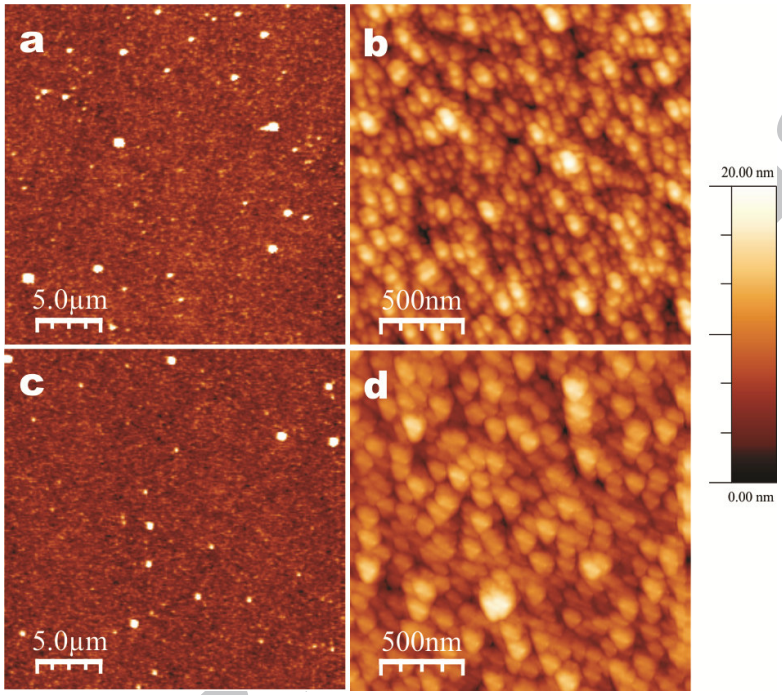

Highlights

- Electropolimerization in ionic liquids
- Ionic exchange in ionic liquid electrolytes
- Electrochemical and electrochromic behavior of polypyrrole in ionic liquids